Colorimetric Iodide Recognition and Sensing by Citrate-Stabilized Core/Shell Cu@Au Nanoparticles

ARTICLE *in* ANALYTICAL CHEMISTRY · MARCH 2011

Impact Factor: 5.64 · DOI: 10.1021/ac200480r · Source: PubMed

5 AUTHORS, INCLUDING:

Jia Zhang
University of Science and Technology of China
39 PUBLICATIONS **477** CITATIONS

SEE PROFILE

analytical chemistry

ARTICLE

pubs.acs.org/ac

Colorimetric Iodide Recognition and Sensing by Citrate-Stabilized Core/Shell Cu@Au Nanoparticles

Jia Zhang, Xiaowen Xu, Cheng Yang, Fan Yang, and Xiurong Yang*

State Key Laboratory of Electroanalytical Chemistry, Changchun Institute of Applied Chemistry, Chinese Academy of Sciences, Changchun 130022

Graduate School of Chinese Academy of Sciences, Beijing 100049, P. R. China

Supporting Information

ABSTRACT: In the light of the significance and urgency for the recognition and sensing of anions specifically, especially those of biological relevance, herein, we wish to demonstrate a novel colorimetric avenue for highly selective iodide recognition and sensing using simple citrate-stabilized core/shell Cu@Au nanoparticles. No other ions than iodide can induce an appreciable color change of the Cu@Au nanoparticles solution from purple to red by transforming the interconnected, irregularly shaped nanoparticles to the single, separated, and nearly spherical ones, as confirmed by the transmission electron microscopy (TEM). On the basis of the optical spectra and TEM studies, a mechanism of iodide-induced aggregating/fusion, fragmentation, and reorganization of atoms is proposed. With this strategy, 6 μM (0.76 ppm) of iodide can be recognized within 20 min by naked-eye observation. This sensitive and selective colorimetric assay opens up a fresh insight of facile, rapid, and reliable detection of iodide and may find its future application in the analysis of the total iodine in edible salt as well as the clinical diagnosis of urinary iodide.

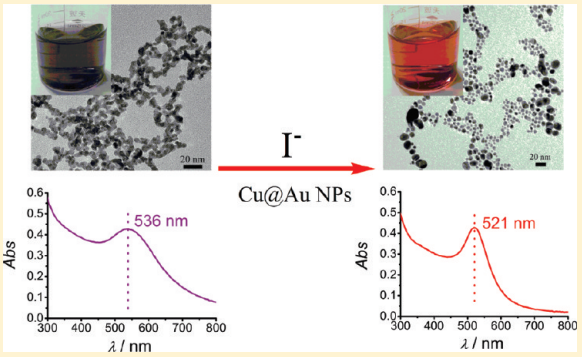

The specific detection of inorganic anions, such as the halide ions, nitrate and nitrite, phosphate, and cyanide, is significant because they are ubiquitous in biological systems and play essential roles in industrial, medical, and environmental processes. Recently, a plethora of chemosensors capable of recognizing, sensing, and separating negatively charged species has been developed by utilizing supramolecular chemistry, which allows one to rationally design new anion-responsive receptors with agreeable or even remarkable selectivities.[1−4] Despite the good selectivity, the use of chemosensors suffers from several drawbacks, such as the complicated organic synthesis procedure involved, water-incompatible properties, and a rather high limit of detection,[5−11] which make anion recognition and sensing a permanent challenge to be explored.

Meanwhile, the determination of anions is usually accomplished by spectroscopic or electrochemical methods upon binding to the specific receptors. Of the spectroscopic detection, the colorimetric way is particularly attractive, due to the quick feedback and facile quantification of signal. Compared to the maturely developed chromogenic chemosensors made with single small molecules for anions, colorimetric sensors based on noble metal nanoparticles (NPs) (e.g., Au and Ag NPs) are very limited and require much more attention to be paid. Two typical NP-based anion-sensing ensembles are exemplified. Au NPs functionalized with nitrite-reactive groups exhibited remarkable selectivity for the detection of nitrite or nitrate ions in a colorimetric way,[12] and Ag nanoplates presented a simple sensing platform in detecting halides, phosphate, and thiocyanate ions in water.[13] Until now, the metal NPs in the development of colorimetric anion sensors are primarily functionalized; thus the challenging question whether simple unmodified NPs can recognize anions specifically arises.

Iodide is of special biological interest due to its confirmed essential roles in neurological activity and thyroid gland function.[14] Either deficiency or abundance of iodide in the thyroid gland can arouse major health concerns. In fact, the World Health Organization (WHO) has stated that iodine deficiency is the biggest cause for mental retardation on a global scale.[15] The other important feature that iodide has is the function to induce depolymerization of actin filaments and a corresponding gel-to-sol state transition.[16] Many fluorescent[17−19] and electrochemical[20−22] sensors for iodide have been developed. Meanwhile, an attractive dual colorimetric and fluorometric system based on a cationic polythiophene derivative has recently been reported for specific iodide assay.[7,23] Despite these achievements, the discrimination of iodide from chemically close anions, particularly by colorimetric means,

Received: February 24, 2011
Accepted: March 30, 2011
Published: March 30, 2011

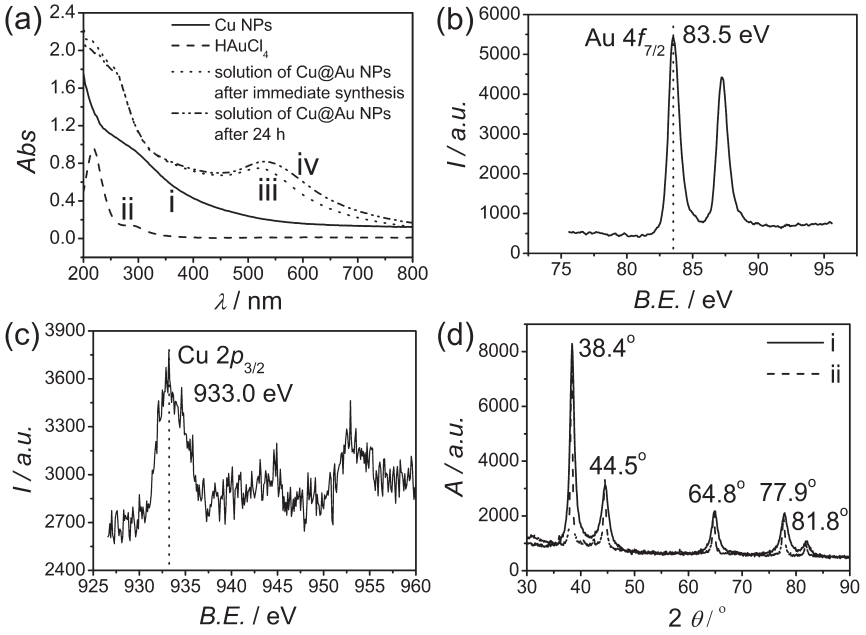

Figure 1. Spectroscopic recordings (a) of the Cu NPs solution (i), $HAuCl_4$ (ii), and Cu@Au NPs solution after immediate synthesis (iii) and 24 h of storage at ambient temperature (iv). XPS spectra of Au 4f (b) and Cu 2p (c) for the Cu@Au NPs. XRD patterns (d) of the native Cu@Au NPs (i) and the reorganized particles (ii) after interaction with 10 μM iodide for 20 min.

requires continual progress, such as to lower the limit of detection and enhance the water-compatible property.

Herein, we demonstrate that iodide anion can be recognized selectively in 100% aqueous solution by colorimetry based on citrate-stabilized core/shell Cu@Au NPs. In our experiment, the addition of iodide unexpectedly induces visible colorimetric response of the Cu@Au NPs solution, the color of which turns from purple to red. This "light-up" colorimetric assay[24,25] has remarkable selectivity, free of interference from all tested metallic cations and most anions. Insofar as we know, this is the first report describing highly specific recognition of an anion by metal NPs without special surface functionalization.[26]

MATERIALS AND METHODS

Reagents. $HAuCl_4 \cdot 3H_2O$, $Cu(NO_3)_2 \cdot 2.5H_2O$, $CuSO_4 \cdot 5H_2O$, and $NaBH_4$ were purchased from Sigma-Aldrich. $AgNO_3$ was purchased from Acros. Analytical grade nickel acetate, cobalt chloride, sodium citrate, sodium iodide, and other chemicals were obtained from Beijing Chemical Reagent Co. They were all used without additional purification. Milli-Q water (18.2 MΩ cm) was used.

Apparatus. UV/vis absorption spectra were recorded with a Cary 50 UV/vis spectrophotometer (Varian, USA). Photographs were taken with a Kodak DX 7590 digital camera. TEM images and EDS results were acquired by using both Hitachi H-800 (Hitachi) and Tecnai G2 F20 (FEI) transmission electron microscopes operated at 200 kV. TEM samples were prepared by applying drops of the NPs solution to carbon-coated copper grids in contact with filter paper. Such a process was made to prevent coagulation of particles. The XPS samples on highly cleaned silicon wafers were analyzed within a spot size of 500 μm by an ESCALAB MK II spectrometer (VG Scientific, UK) with Al Kα radiation as the X-ray source and a pass energy of 100 eV. Peak positions were internally referenced to the C1s peak at 284.6 eV. XRD patterns were recorded on square glass slides by a D/Max 2500 V/Pc X-ray diffractometer (Rigaku) with a Cu Kα radiation of 40 kV and 40 mA. The ζ-potential of the NPs was examined by a Malvern Zetasizer instrument (Malvern). The electrochemical experiments were carried out on a CHI 660B electrochemical workstation (Shanghai Shenhua Apparatus) in a homemade one-compartment cell by standard three-electrode systems. A Ag/AgCl (sat. KCl) electrode was used as the reference electrode, a Pt foil as the counter electrode, and the ITO slide, which was sealed by a "O-ring" with 6 mm inner diameter, as the working electrode.

Synthesis Procedure. In a typical experiment (12 ± 1 °C), 20 mL of water was added with aqueous solutions of $CuSO_4$ (50 μL, 0.1 M) and sodium citrate (50 μL, 0.1 M). Afterward, 1 mL of freshly prepared $NaBH_4$ (3.8 mg in 4 mL of H_2O) was injected into the stirring system rapidly. About 15 min later, aqueous $HAuCl_4$ solution (50 μL, 0.1 M) was added, and the solution was kept stirring for 20 min. The final solution was stored at ambient environment (14 ± 2 °C) for 24 h before its further applications.

RESULTS AND DISCUSSIONS

Synthesis and Characterization of Cu@Au NPs. We suppose that the synthesis involves the combination of a galvanic displacement reaction between $HAuCl_4$ and Cu NPs and reduction of $HAuCl_4$ by the remaining $NaBH_4$ after generation of Cu NPs. Three analytical techniques were combined to elucidate the chemical structure of the product. It was first characterized by UV−vis spectra (Figure 1a). The yellow Cu NPs solution displayed no surface plasmon resonance (SPR) band in the visible spectra range (Figure 1a, i), suggesting the NPs were less than 2 nm in diameter.[27] On the addition of $HAuCl_4$, the solution turned wine red immediately, indicating a prompt growth of Au shell onto the Cu NPs core. After reaction, the absorbance of

dx.doi.org/10.1021/ac200480r |*Anal. Chem.* 2011, 83, 3911–3917

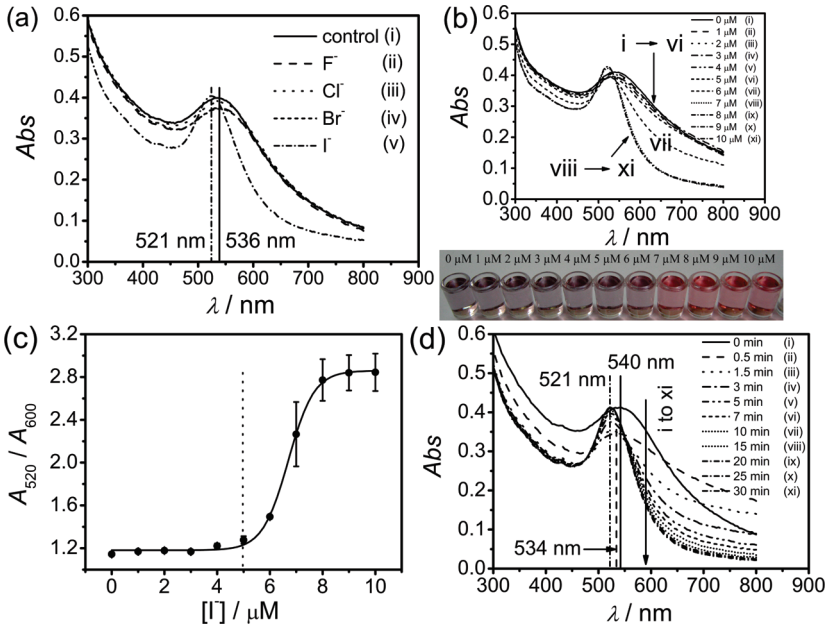

Figure 2. (a) Absorption profiles of Cu@Au NPs solution (pH 5.2) in the absence (i) and presence of halides (ii−v) for 20 min. (b) Absorption profiles of Cu@Au NPs solution (pH 5.2) after interaction with different amounts of iodide ion (0−10 μM) for 20 min (upper part) and an instant photograph showing the colorimetric change (down part). (c) The A_{520}/A_{600} ratio as a function of iodide concentration. (d) Time-dependent absorption spectra of Cu@Au NPs solution (pH 5.2) on the addition of 10 μM iodide.

$HAuCl_4$ centered at 218 and 293 nm (Figure 1a, ii) vanished, and a new absorbance band featuring gold SPR emerged at 520 nm[28] (Figure 1a, iii), suggesting a complete transformation of $AuCl_4^-$ to clusters of Au atoms, with an average size above 2 nm. It can be impossible only with the displacement reaction because it just took place on the outermost layer of Cu NPs, thus providing unambiguous evidence for the reduction of $AuCl_4^-$ by $NaBH_4$. The new gold SPR band was extended to 530 nm and became a little more intense within 24 h (Figure 1a,iv), suggesting some aggregation of the Cu@Au NPs. Afterward, the solution remained stable for at least 2 weeks when stored at room temperature (14 ± 2 °C).

The coverage of Au atoms on Cu NPs was further confirmed by X-ray photoelectron spectroscopic (XPS) analysis. The binding energy (E_B) for Au $4f_{7/2}$ was located at 83.5 eV, consistent with the zero-valence of Au atoms (Figure 1b). One can see the blue-shift of E_B for Au $4f_{7/2}$ when compared to that of bulk gold atom (83.9 eV),[29] probably due to an electronic modification of the Au atoms by Cu NPs. The Cu 2p spectrum exhibited a E_B at 933.0 eV associated with Cu $2p_{3/2}$ (Figure 1c), which is assumed to be ascribed to metallic Cu (Cu^0).[30] Additionally, it clearly showed separate broad peaks around 939−945 eV, which should be resulted from the generation of Cu^{2+} ions[31] by the displacement reaction. To better give insight to the core/shell structure of the Cu@Au NPs, X-ray diffraction (XRD) data were collected (Figure 1d, i). The XRD pattern showed five 2θ peak positions (38.4°, 44.5°, 64.8°, 77.9°, and 81.8°), which corresponded to the {111}, {200}, {220}, {311}, and {222} lattice planes of the face-centered cubic (fcc) lattice of pure gold. No shift of the reflections to higher angle indicative of alloy formation was observed, identifying definitively the core/shell nature of the NPs. In addition, the pattern did not show separate reflections of metallic Cu, which can be accounted for by the ultrasmall size of the Cu core.[32]

UV−Vis Spectroscopic and Transmission Electron Microscopic (TEM) Observations. A colorimetric test for iodide recognition was conducted in phosphate buffer solution (PBS, pH 5.2) at room temperature. It can be clearly seen that none other than iodide induced an exciting change of the absorption spectra of the NPs solution (Figure 2a). The peak position relative to the gold SPR band shifted from 536 to 521 nm and the bandwidth dramatically decreased. Correspondingly, the color of the solution changed from purple to red. It is expected that size, shape, degree of aggregation, and dielectric environment of the Cu@Au NPs are associated with the present phenomena.[33−36] Such highly specific discrimination of iodide from other halides by the simple Cu@Au NPs is exhilarating and unexpected. Similar recognition was observed with KI rather than NaI and with Cu@Au NPs when the $CuSO_4$ was replaced by $Cu(NO_3)_2$ in the synthesis. Several control experiments were performed. We exchanged the Cu NPs core with Ag, Co, or Ni NPs, but the obtained NPs failed to recognize iodide; thus, no visible color change occurred. We also studied the recognition ability of pure citrate-stabilized Au NPs, and the result was still negative. In addition, $HAuCl_4$ was replaced by $AgNO_3$ to the synthesis of core/shell Cu@Ag NPs. The formed NPs were found to be iodide-responsive; however, they could also respond to chloride and bromide ions. From the above investigations, it is clear that both the Cu NPs core and the Au atoms shell are responsible for the highly specific recognition of iodide.

Encouraged by the amazing phenomenon, we then explored the function of iodide ion concentration on the optical spectra of the NPs solution. Changes in the gold plasmon band upon the addition of 10 μM iodide were discovered the same as those of 100 μM iodide. Spectroscopic results (pH 5.2, 20 min) correlated with the iodide concentration (0−10 μM), as shown in Figure 2b (upper part). With the addition of iodide from 0 to 5 μM, the plasmon bandwidth barely changed, while the peak position shifted negatively from 540 to 530 nm (Figure 2b, i−vi). At 6 μM, the optical spectrum separated from the others by a dramatic decrease of plasmon bandwidth. In addition, the

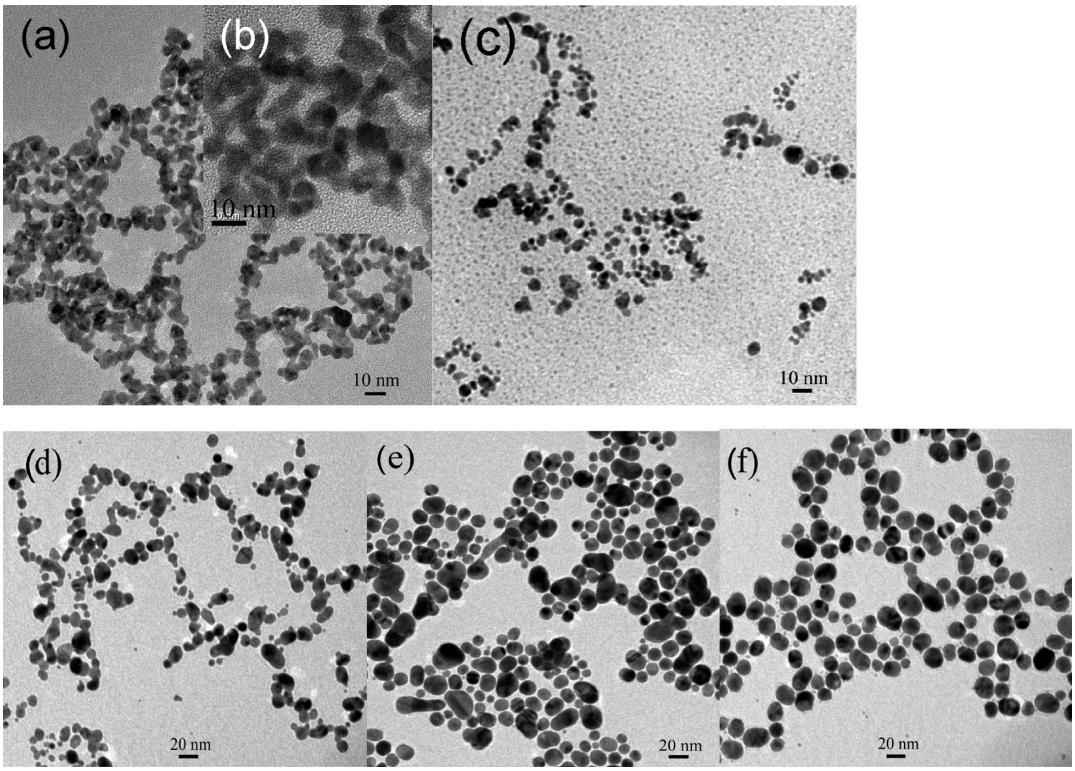

Figure 3. Representative TEM images of Cu@Au NPs before (a, b) and after interaction with iodide ion for 20 min corresponding to concentrations of 5 μM (c), 6 μM (d), 8 μM (e), and 10 μM (f), respectively.

peak position continued to move to 527 nm (Figure 2b, vii). Above 7 μM (included), the optical spectra kept stable, having the minimum plasmon bandwidth and the peak position centered at 521 nm (Figure 2b, viii−xi), suggesting that the interaction between iodide and Cu@Au NPs reached an end point. This spectra transition can be alternatively revealed by the color change of the solution (Figure 2b, bottom), from purple (0−5 μM) through purple reddish (6 μM) to red (above 7 μM). It should be mentioned that the onset of the color change varied a little (6 ± 1 μM) according to five parallel experiments. A sigmoid function curve was obtained by correlating the ratio of absorbance measured at 520 and 600 nm (A_{520}/A_{600}) with iodide ion concentration (Figure 2c), in which the onset of the ratio change is in accordance with the spectroscopic results and the solution color change. The limit of detection (LOD) was estimated to be 5 μM. This detection limit is much lower than those of comparable anion sensors based on group-functionalized metal NPs.[12,37,38] Interference tests were made (Figure S1, Supporting Information). All the tested ions could not lead to similar absorbance or color change as iodide did. This result highlights the remarkably specific recognition of iodide by the Cu@Au NPs. Meanwhile, the optical response or solution color change resulting from iodide was little affected by the coexistence of most of ions, except S^{2-}, $S_2O_3^{2-}$, and Fe^{2+} ions. It should be admitted that the recognition event was greatly interfered by all of the metallic ions when their concentration reached 1 mM, due to their interaction with the citrate ions. Nevertheless, the disturbing situation can be perfectly settled by the replacement of citrate ions with some *certain* polymer, such as dextran, to stabilize the NPs before the recognition, or by screening the cations with a strong chelating agent, such as EDTA.

This iodide amount dependent spectroscopic observation was assisted by the transmission electron microscopy (TEM) studies (Figure 3) to give insight into the influence of iodide on the geometry of Cu@Au NPs. The native particles are nonspherical, interconnected in shape, having an average size of 10 nm (Figure 3a,b), which agreed well with the size (9.3 nm) estimated by XRD data according to the Debye−Scherrer equation. Similar morphology was observed for the PB@Pt clusters, which relied on the catalytic growth of Prussian Blue shells onto the surface of Pt NPs.[39] On the basis of the TEM image and the high reactivity of Cu NPs and $NaBH_4$, we suppose that the nucleation and growth of Au layers would occur quickly enough to encapsulate several Cu NPs in a single Cu@Au NP. When a small amount of iodide (5 μM) was added, the NPs appeared more spherical than the original ones, and there emerged a large part of small particles with a diameter of 2−10 nm, some even below 2 nm. However, some larger particles with a diameter above 10 nm were also observed (Figure 3c). On the addition of 6 μM iodide, an increased proportion of spherical particles was seen, with the size being predominantly in the range of 10−20 nm (Figure 3d). A further increase of iodide (8, 10 μM) led to nearly spherical, well-dispersed particles with an average diameter of 20 nm (Figure 3e,f), and this effect was more profound at 10 μM iodide (Figure 3f). Comparison of the spectroscopic responses with the corresponding TEM results reveals that the blue-shift of the gold SPR band and the reduction in the $\Delta\lambda$ are actually correlated with the variation in size, shape, degree of aggregation, and even dielectric environment of the Cu@Au NPs.[33−36] In other words, the combined influence from these changes dictates optical responses in the presence of iodide.

It is of importance to understand that the interaction of iodide and Cu@Au NPs is also time-dependent. The kinetic process

dx.doi.org/10.1021/ac200480r |*Anal. Chem.* 2011, 83, 3911–3917

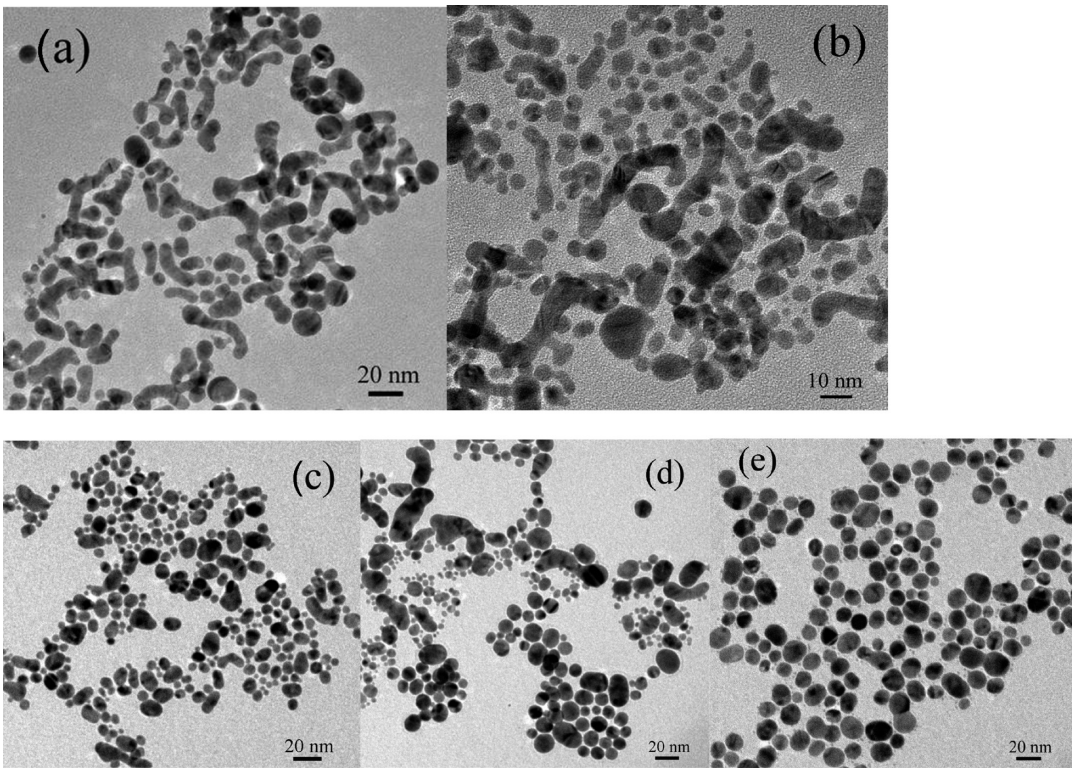

Figure 4. Time-dependent TEM images of Cu@Au NPs after addition of 10 μM iodide for about 0.5 min (a, b), 3 min (c, d), and 10 min (e), respectively.

upon the addition of 10 μM iodide was spectroscopically evaluated, as shown in Figure 2d. After a short 0.5 min, the gold SPR band became widen and the peak height decreased, while the peak position blue-shifted by 6 nm, from 540 to 534 nm (Figure 2d, i,ii). With progression of the interaction, the $\Delta\lambda$ gradually reduced, the peak height increased, and the peak position remained stable at 521 nm after 1.5 min (Figure 2d, iii−xi). The change of the A_{520}/A_{600} ratio with time shows that the interaction almost finished within 20 min (Figure S2, Supporting Information). TEM examination was performed to assist the understanding of this optical observation. Compared to the native Cu@Au NPs, the particles after 0.5 min interaction were more irregular in geometry and better separated (Figure 4a,b). Moreover, in some domains we found some particles spherical in shape and smaller than 10 nm in diameter (Figure 4b). After 3 min, more regular, spherical particles emerged, but with a wide size distribution (Figure 4c,d). Besides, a large amount of very small particles appeared by the side of both irregular and spherical particles (Figure 4d). After further prolonging to 10 min, nearly spherical particles with an average size of 15 nm were observed (Figure 4e).

Mechanism of the Iodide Recognition. This dimensional evolution of the Cu@Au NPs on the addition of iodide is naturally reminiscent of the iodide-induced morphological transformation of Au NPs, as discovered by Cheng et al.[35] and Wang et al.[40] Both authors demonstrated the occurrence of chemisorption of iodide on Au NPs, which they believed can increase van der Waals attractive forces between NPs by lowering the surface potential and then induce the fusion, fragmentation, and aggregation of NPs in the solution. They also mentioned the comparable role of electron injection by the reductive chemisorption of iodide ions ($I^- \rightarrow I_{(adsorbed)} + e^-$) playing on the dimensions of NPs to other energetic injection processes.[41−44] Nevertheless, the distinctly different optical responses and TEM results indicate that iodide interaction in our system must follow another pathway. On the other hand, Kapoor and the co-workers discovered that stable Cu NPs could be obtained in the presence of iodide ions under aerated conditions.[45] The iodide ions were adsorbed on the surface of Cu NPs for stabilization. Therefore, on the basis of our experimental data and those previous illuminating studies,[35,40−44] a mechanism of iodide-induced aggregating/fusion, fragmentation, and reorganization of atoms is proposed, as represented in Scheme 1. The iodine atoms that are spontaneously adsorbed on the pseudocore/shell Cu@Au clusters (Scheme 1a) will neutralize surface charge by displacing the stabilizing citrate ions. The reduction in ζ-potential triggers aggregating/fusion of the clusters, which must be accompanied by inclusion and adsorption of iodide ions on the surface of Cu cores (Scheme 1b). As a result of the inclusion, the ζ-potential of the fusing intermediate increases dramatically, which would reversely lead to *prompt* fragmentation, thus producing smaller clusters and ultrasmall gold particles (Scheme 1c,d). With progression of fragmentation, the number of the intermediate becomes less, in accompaniment with the reorganization of atoms forming more spherical, larger particles (Scheme 1e). However, according to the XRD result, no alloy or larger pure Cu NPs (size above 2 nm) will be expected, since only gold reflections were detected (Figure 1d, ii). It can be conceivable that this reorganization process is similar to Ostwald ripening, by which particles grow larger at the sacrifice of smaller ones, and higher iodide concentration can accelerate the ripening process. The iodine atoms resulting from the chemisorptive reduction of iodides were identified by XPS studies, electrochemistry, and optical spectra (Figure S3−S5, Supporting Information). As reference, the EB

Scheme 1. Schematic Representation of Morphological Transformation of Cu@Au NPs upon the Addition of Iodide[a]

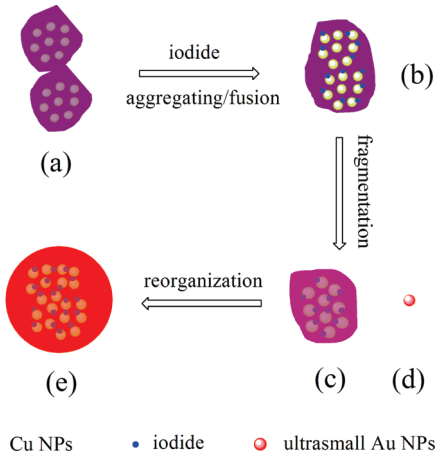

[a] The purple and red parts represent clusters of Au atoms.

for I 3d5/2 in NaI is 619.1 eV. After interaction, the EB moved negatively to 618.3 and 618.4 eV for 5 and 10 μM iodide cases, respectively, which are a signature of zerovalent iodine atoms.[29] Moreover, the Au 4f7/2 and Cu 2p3/2 peak positions were barely changed, suggesting no variation in their oxidation state. A quantitative analysis showed a gradual decrease of the ratio of Cu to Au (Cu/Au) from 0.27 (native Cu@Au NPs) through 0.20 (case of 5 μM iodide) to 0.12 (case of 10 μM iodide). This result predicts the increase of surface Au atoms layer and the resultant decrease in the detected Cu amount, supporting the presence of reorganized particles. Electrochemical studies were conducted on native Cu@Au NPs and reorganized NPs (10 μM iodide) with modified ITO (indium−tin oxide) electrodes. After interaction of iodide and Cu@Au NPs, a new broad peak at around 1.2 V appeared, which can be marked as the characteristic oxidation voltammetry of iodine to iodate.[46] The chemisorption of iodide was also corroborated by the absorption changes that took place at the 226 nm, where iodide has a charge-transfer-to-solvent (CCTS) band in aqueous solution. This band was not present in the 10 μM iodide case, while it appeared at the higher iodide concentrations (20−50 μM). The former shows that iodide lost its CTTS band upon chemisorption, and the latter explains that this chemisorption of iodide reached the end point within 20 μM, supporting the colorimetric results (vide supra). The inclusion of iodide played a crucial role in the stabilization of reorganized NPs. We found that the ζ-potentials of the NPs were −20.7, −33.6, and −35.1 mV in the absence and presence of 5 and 10 μM iodide, respectively. The more negative ζ-potential cannot be explained by the generation of $[AuI_2]^-$ complex, since the oxidation state of Au did not change (vide supra). The only reasonable explanation is that iodide ions were included and bound to the surfaces of the Cu cores.

pH Effect. It should be noted that the oxidation of iodide on the surface of Au atoms is coupled to proton reduction,[47] suggesting a connection of the recognition behavior to the pH environment. The influence of solution pH value was studied at 10 μM iodide for 20 min interaction, as shown in Figure 5. One can observe a dramatic optical change at the pH transition of 6.0 to 7.0, which can be alternatively mirrored by the function curve of the A_{520}/A_{600} ratio versus pH or the solution color change from red to purple reddish (Figure S6, Supporting Information).

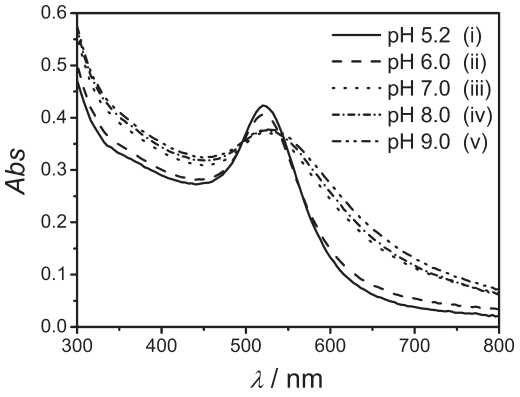

Figure 5. pH-dependent optical spectra of Cu@Au NPs solution on the addition of 10 μM iodide for 20 min.

The function curves of the A_{520}/A_{600} ratio with the iodide concentration for pH 6.0 to 9.0 showed the LODs being 7, 8, 9, and 9 μM, respectively (Figure S7, Supporting Information).

CONCLUSION

In summary, we have presented a novel colorimetric way for the visual detection of iodide using simple citrate-stabilized core/shell Cu@Au NPs. No other ions than iodide can induce the visible color change of the NPs solution from purple to red by transforming the original nonspherical clusters of particles to single, spherical, larger ones. This highly iodide-specific recognition suffers insignificant interference from most of the tested ions, and the sensitivity is much better than those of other anion sensors using functionalized NPs. On the basis of the optical observations and TEM examinations, an aggregating/fusion, fragmentation, and reorganization of atoms mechanism was proposed. The solution pH environment exerts influence on the sensitivity of the colorimetric iodide assay. The experimental results reported here open up an innovative insight of facile, rapid, and reliable diagnosis of iodide, thus paving the way for the development of a simple, label-free, and selective colorimetric way for other anions in aqueous solution based on the Cu@Au NPs. Moreover, it is highly expected for this solution-based laboratory assay to develop into a type of paper-based test kit[48] for point-of-care applications.

ASSOCIATED CONTENT

Supporting Information. Additional information as noted in the text. This material is available free of charge via the Internet at http://pubs.acs.org.

AUTHOR INFORMATION

Corresponding Author

*E-mail: xryang@ciac.jl.cn. Fax: +86 431 85269278.

ACKNOWLEDGMENT

This work was supported by the National Natural Science Foundation of China (No. 20890020) and the National Key Basic Research Development Project of China (No. 2010CB933602; 2007CB714500).

REFERENCES

(1) Beer, P. D.; Gale, P. A. *Angew. Chem., Int. Ed.* **2001**, *40*, 486.
(2) Katayev, E. A.; Ustynyuk, Y. A.; Sessler, J. L. *Coord. Chem. Rev.* **2006**, *250*, 3004.
(3) Kim, S.; Lee, D.; Hong, J.; Yoon, J. *Acc. Chem. Res.* **2009**, *42*, 23.
(4) Caltagirone, C.; Gale, P. A. *Chem. Soc. Rev.* **2009**, *38*, 520.
(5) Black, C. B.; Andrioletti, B.; Try, A. C.; Ruiperez, C.; Sessler, J. L. *J. Am. Chem. Soc.* **1999**, *121*, 10438.
(6) Sancenon, F.; Martinez-Manez, R.; Soto, J. *Angew. Chem., Int. Ed.* **2002**, *41*, 1416.
(7) Ho, H.; Leclerc, M. *J. Am. Chem. Soc.* **2003**, *125*, 4412.
(8) Cho, E.; Moon, J.; Ko, S.; Lee, J.; Kim, S.; Yoon, J.; Nam, K. *J. Am. Chem. Soc.* **2003**, *125*, 12376.
(9) Jimenez, D.; Martinez-Manez, R.; Sancenon, F.; Ros-Lis, J. V.; Benito, A.; Soto, J. *J. Am. Chem. Soc.* **2003**, *125*, 9000.
(10) Vazquez, M.; Fabbrizzi, L.; Taglietti, A.; Pedrido, R. M.; Gonzalez-Noya, A. M.; Bermejo, M. R. *Angew. Chem., Int. Ed.* **2004**, *43*, 1962.
(11) Hudnall, T. W.; Gabbai, F. P. *J. Am. Chem. Soc.* **2007**, *129*, 11978.
(12) Daniel, W. L.; Han, M.; Lee, J.; Mirkin, C. A. *J. Am. Chem. Soc.* **2009**, *131*, 6362.
(13) Jiang, X.; Yu, A. *Langmuir* **2008**, *24*, 4300.
(14) Malongo, T. K.; Patris, S.; Macours, P.; Cotton, F.; Nsangu, J.; Kauffmann, J. *Talanta* **2008**, *76*, 540.
(15) http://www.iccidd.org.
(16) Kabir, S. R.; Yokoyama, K.; Mihashi, K.; Kodama, T.; Suzuki, M. *Biophys. J.* **2003**, *85*, 3154.
(17) Kim, H.; Kang, J. *Tetrahedron Lett.* **2005**, *46*, 5443.
(18) Okamoto, H.; Konishi, H.; Kohno, M.; Satake, K. *Org. Lett.* **2008**, *10*, 3125.
(19) Lin, W.; Yuan, L.; Cao, X.; Chen, B.; Feng, Y. *Sens. Actuators B* **2009**, *138*, 637.
(20) Malon, A.; Radu, A.; Qin, W.; Qin, Y.; Ceresa, A.; Maj-Zurawska, M.; Bakker, E.; Pratsch, E. *Anal. Chem.* **2003**, *75*, 3865.
(21) Pereira, F. C.; Fogg, A. G.; Ugo, P.; Bergamo, E. P.; Stradiotto, N. R.; Zanono, M. V. B. *Electroanalysis* **2005**, *17*, 1309.
(22) Pereira, F. C.; Moretto, L. M.; Leo, M. D.; Zanono, M. V. B.; Ugo, P. *Anal. Chim. Acta* **2006**, *575*, 16.
(23) Wang, J.; Zhang, Q.; Tan, K.; Long, Y.; Ling, J.; Huang, C. *J. Phys. Chem. B* **2011**, *115*, 1693.
(24) Liu, J.; Lu, Y. *J. Am. Chem. Soc.* **2005**, *127*, 12677.
(25) Liu, J.; Lu, Y. *Angew. Chem., Int. Ed.* **2006**, *45*, 90.
(26) Even though the unmodified silver nanoplates the authors in ref 4 employed could distinguish halides, phosphate, and thiocyanate ions from other anions and metallic cations, they can hardly discriminate the three kinds of anions from each other.
(27) Celep, G.; Cottancin, E.; Lerme, J.; Pellarin, M.; Arnaud, L.; Huntzinger, J. R.; Vialle, J. L.; Broyer, M.; Palpant, B.; Boisron, O.; Melinon, P. *Phys. Rev. B* **2004**, *70*, 165409.
(28) In fact, the newly emerged gold SPR band varied from 510 to 520 nm, according to five parallel experiments.
(29) Bravo, B. G.; Michelhaugh, S. L.; Soriaga, M. P.; Villegas, I.; Suggs, D. W.; Stickney, J. L. *J. Phys. Chem.* **1991**, *95*, 5245.
(30) Kim, M.; Na, H.; Lee, K.; Yoo, E.; Lee, M. *J. Mater. Chem.* **2003**, *13*, 1789.
(31) Tominaga, M.; Taema, Y.; Taniguchi, I. *J. Electroanal. Chem.* **2008**, *624*, 1.
(32) Sarkar, A.; Manthiram, A. *J. Phys. Chem. C* **2010**, *114*, 4725.
(33) Takeuchi, Y.; Ida, T.; Kimura, K. *J. Phys. Chem. B* **1997**, *101*, 1322.
(34) Link, S.; El-Sayed, M. A. *J. Phys. Chem. B* **1999**, *103*, 4212.
(35) Cheng, W.; Dong, S.; Wang, E. *Angew. Chem., Int. Ed.* **2003**, *42*, 449.
(36) Kelly, K. L.; Coronado, E.; Zhao, L.; Schatz, G. C. *J. Phys. Chem. B* **2003**, *107*, 668.
(37) Watanabe, S.; Seguchi, S.; Yoshida, K.; Kifune, K.; Tadaki, T.; Shiozaki, H. *Tetrahedron Lett.* **2005**, *46*, 8827.
(38) Kumar, A.; Chhatra, R. K.; Pandey, P. S. *Org. Lett.* **2010**, *12*, 24.
(39) Zhang, J.; Yang, W.; Zhu, H.; Li, J.; Yang, F.; Zhang, B.; Yang, X. *J. Colloid Interface Sci.* **2009**, *338*, 319.
(40) Wang, J.; Li, Y.; Huang, C. *J. Phys. Chem. C* **2008**, *112*, 11691.
(41) Kurita, H.; Takami, A.; Koda, S. *Appl. Phys. Lett.* **1998**, *72*, 789.
(42) Chang, S.; Shih, C.; Chen, C.; Lai, W.; Wang, C. *Langmuir* **1999**, *15*, 701.
(43) Link, S.; Burda, C.; Nikoobakht, B.; El-Sayed, M. A. *J. Phys. Chem. B* **2000**, *104*, 6152.
(44) Jin, R.; Cao, Y.; Mirkin, C. A.; Kelly, K. L.; Schatz, G. C.; Zheng, J. *Science* **2001**, *294*, 1901.
(45) Kapoor, S.; Joshi, R.; Mukherjee, T. *Chem. Phys. Lett.* **2002**, *354*, 443.
(46) Finklea, H. O. In *Electroanalytical Chemistry*; Bard, A. J. , Ed.; Marcel Dekker: New York, 1996; Vol. 19, pp 185−187.
(47) Mulvaney, P. *Langmuir* **1996**, *12*, 788.
(48) Zhao, W.; Ali, M. M.; Aguirre, S. D.; Brook, M. A.; Li, Y. *Anal. Chem.* **2008**, *80*, 8431.